

Self-Assembly of Patchy Particles

Zhenli Zhang[†] and Sharon C. Glotzer^{*,†,‡}

*Departments of Chemical Engineering and Materials Science and Engineering,
University of Michigan, Ann Arbor, Michigan 48109-2136*

Received May 1, 2004; Revised Manuscript Received June 8, 2004

ABSTRACT

Molecular simulations are performed to study the self-assembly of particles with discrete, attractive interaction sites – “*patches*” – at prescribed locations on the particle surface. Chains, sheets, rings, icosahedra, square pyramids, tetrahedra, and twisted and staircase structures are obtained through suitable design of the surface pattern of patches. Our simulations predict that the spontaneous formation of two-dimensional sheets and icosahedra occurs via a first-order transition while the formation of chains occurs via a continuous disorder-to-order transition as in equilibrium polymerization. Our results show how precise arrangements of patches combined with patch “recognition” or selectivity may be used to control the relative position of particles and the overall structure of particle assemblies. In this context, patchy particles represent a new class of building block for the fabrication of precise structures.

Next generation materials and devices composed of nanoscopic building blocks tailor-made for specific applications will not be fabricated via traditional methods. Instead, they will self-assemble through processes that do not require human intervention and in which instructions for assembly emerge from the nature of the forces acting between constituents. In traditional self-assembled materials such as block copolymers and surfactants, free energy minimization drives the emergence of structures that are often polydisperse and irregular. In contrast, biological molecules such as virus capsid proteins assemble into highly monodisperse and precise structures such as icosahedra in HIV (human immunodeficiency virus) and helical cylinders in tobacco mosaic virus. Future materials and devices for photonics, molecular electronics, drug delivery devices, and sensors require the self-assembly of synthetic nanostructures with the precision and reliability of biological self-assembly. Despite enormous advances in the synthesis of a wide assortment of inorganic and organic nanoscopic building blocks of various shapes and sizes, such as quantum dots,¹ semiconducting nanorods,² and Buckyballs,³ control over their assembly into precise and predictable structures such as sheets, shells, and wires remains the primary obstacle to the bottom-up construction of novel materials and devices from these building blocks. Attaining such control requires several achievements, most notably elucidating the interactions between nano building blocks, gaining control over these interactions, and understanding how specific types of interactions lead to specific target structures.

One emerging approach to confer upon nanoparticles predetermined “instructions” for assembly is to anisotropically decorate the surface of the particles with synthetic organic or biological molecules. This strategy may be considered biologically inspired because it takes the concepts abstracted from self-assembly of biological systems, where the precision of assembled structures originates in the precision of the interactions between the constituents, and applies them to the self-assembly of particles into specific structures and working devices.⁴

Several examples of this type of directional assembly may be found in the literature. For example, polyhedral, plate-like gold particles with chromium- or platinum-coated faces were functionalized by hydrophobic CH₃-terminated self-assembled monolayers (SAMs) or hydrophilic OH-terminated SAMs.⁵ When the particles are added to water, the hydrophobic surfaces organize so as to minimize their contact with the surrounding liquid, which drives the particles to assemble into highly organized one-, two- and three-dimensional structures. Due to the specific shape of the particles and the asymmetric interactions patterned on their surface, the interactions between particles are selective and directional, resulting in assembled structures with substantially fewer defects than via conventional self-assembly methods. Because of experimental limitations in decorating particles with precise patterns of interactions, most of the examples in the literature are limited to particles of micrometer and millimeter size. Recently, however, great progress has been made in patterning the surfaces of nanoparticles to more precisely control their interactions. For example, Janus particles have been made by evaporating gold films onto hemispheres of 100–500 nm diameter silica colloids.^{6,7} Gold and silver nanoparticles of ~4 nm diameter have been synthesized with

* Corresponding author. E-mail: sglotzer@umich.edu.

[†] Department of Chemical Engineering.

[‡] Department of Materials Science and Engineering.

mixtures of ligands that self-assemble on the particle surface into regular patterns as small as 5 Å, imparting a controllable, repeating pattern of hydrophobic and hydrophilic interactions to the surfaces of nanoparticles.⁸

There are also many examples of functionalizing the surfaces of nanoparticles with DNA oligonucleotides, genetically engineered proteins, and antibody/antigen pairs.^{9–11} The complementarity of these biomolecules provides a “lock-and-key” specificity that has been used to direct the assembly of nanoparticles into aggregates by changing temperature, solvent pH, salt concentration, and other variables. The structures of these aggregates, however, have not yet reached the level of complexity characteristic of biological structures. Nor are they as complex as the structures (e.g., wires, sheets, shells) needed for many nanotechnology applications. Two major factors in this lack of higher order appear to be the imprecision in the number and location of the ligands on the nanoparticle surface and the lack of offsetting forces capable of positioning the agglomerated particles relative to one another.^{11a}

Even in the absence of ligand functionalization, “patchy” interactions may arise between nanoparticles. For example, in nanoparticle synthesis, the nanoparticle size and shape are often controlled by stabilizers such as thiols, phosphines, or carboxylic acids. Recent studies indicate that the distribution of organic molecules within the stabilizer coating is anisotropic and inhomogeneous,^{12–17} and observations of the spontaneous assembly of nanoparticles into highly ordered structures have been reported. For example, Kotov and co-workers observed the spontaneous formation of wires, chains, and sheets in suspensions of thiol-coated CdTe nanoparticles^{12,17} and attributed this to inhomogeneities – patchiness – in the coating. Additionally, the geometry of small particles, which can deviate significantly from a generic spherical shape, can induce orientation-specific interactions at nanometer scales.¹⁸ It has been argued that exceptionally large dipole moments arising apparently from the nearly tetrahedral shape of small CdSe or CdTe nanoparticles in water induces their self-assembly into chains and rings,^{17,19–21} reminiscent of certain assembled protein structures.²²

From a theoretical standpoint, all of these (either intentionally or unintentionally) “patterned” particles may be viewed as a general class of particles interacting with strongly anisotropic, highly directional interactions in which effectively attractive “patches” induce the assembly of otherwise neutral or repulsive particles into ordered structures. This class of “patchy particles” also contains some natural, biological macromolecules, for example, globular proteins, which, to crude first approximation, may be described by otherwise non- or weakly interacting particles with hydrophobic, effectively attractive, patches. In all cases, the extent of the atoms or molecules comprising the patches is smaller than the size of the particles, and the patches are discrete and limited in number. In appropriate solvent conditions, particles will organize themselves to maximize favorable, and minimize unfavorable, contacts between them. The primary challenge for nanotechnology is then to ascertain precisely

what structures will form from nanoparticles with a particular surface pattern of attractive and repulsive interactions.

In this paper, we propose a simplified model of patchy particles suitable for simulation of particles of arbitrary shape, and carry out a series of simulations to investigate the relationship between interaction “patchiness”, particle shape, and the self-assembly of target structures from small numbers of particles. We demonstrate that specific arrangements of attractive patches may be used to direct the organization of particles from a disordered state into unique structures such as chains, sheets, rings, and icosahedra. Our results suggest that the strategy of decorating the surfaces of particles in precise patterns with molecules whose interaction promotes an anisotropic association among particles may indeed provide a potentially universal way to rationally self-assemble particles into predictable, precise, ordered structures.

Here we propose a “minimal” model of particles interacting with strongly anisotropic, directional interactions arising from discrete, attractive patches on the particle surface. Because self-assembly typically requires long simulation times, it is computationally necessary to use a coarse-grained model in which groups of atoms within the particles are represented by a single, coarse-grained “atom”, thereby greatly reducing the overall number of forces that must be computed for each time step while retaining enough granularity to represent the patchiness of the interactions. In our model, particles are composed of spherical subunits (“atoms”) of diameter σ , separated by a distance $l = \sigma$, frozen into the desired particle geometry. For computational efficiency, only the outermost layer of surface “atoms” is retained and the internal “atoms” are not considered. An example of a spherical particle with two, diametrically opposed, attractive “patches” is shown in Figure 1a (patches are colored red). The interactions between experimentally realizable patchy particles are diverse because they depend on the material comprising the patches, particles and solvent. The particles we consider may contain tens to millions of atoms depending on their size and composition, and the patches may represent, e.g., as few as one or several complementary biomolecules or as many as thousands of organic molecules that interact via van der Waals forces, again depending upon the particular system considered.

Here we seek to understand general features of self-assembly, rather than to model any one specific system. To this end we apply empirical pair potentials between “atoms” that model weak, long-range attractive (Lennard-Jones characterized by interaction “strength” ϵ) and excluded-volume (soft-sphere, Weeks–Chandler–Anderson) interactions.^{23–25} For selective patches composed of, e.g., associating organic ligands or complementary molecules such as DNA,⁹ the “atoms” within the patches are of two types with attractive interaction only among atoms on other particles of the same or complementary type. In this way, recognition and directionality are imparted to the interactions.

Several models exist that consider the effect of directionality of short-ranged attractive interactions of particles on bulk phase behavior.^{26–29} These models have in common the introduction of a single artificial potential that depends on

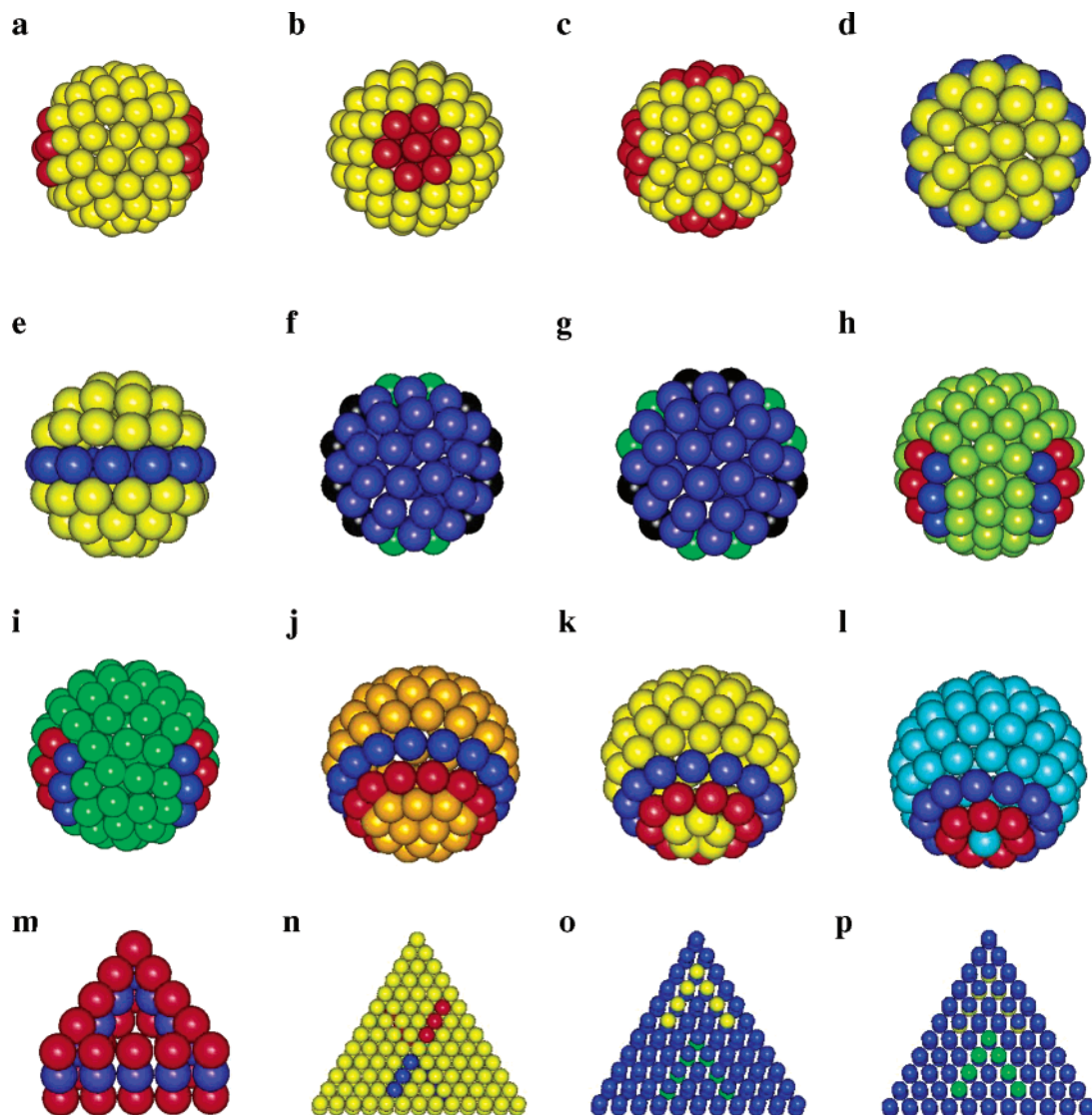


Figure 1. Model patchy particles studied in this work. (a) Side view of patchy sphere with two diametrically opposed circular patches. Red beads represent coarse-grained “atoms” in the patches. Yellow beads represent the rest of the particle. (b) Axial view of the patchy sphere in 1a. (c) Patchy sphere with four circular patches arranged in an equatorial plane on the four vertices of a square. (d) Axial view of sphere with ring-like patch on the equator. (e) Side view of the ring-like patch in 1d. (f) Axial view of patchy sphere with patterned ring-like patch. (g) Axial view of patchy sphere with patterned ring-like patch. Note the pattern of the patch is different from 1f. (h) Patchy sphere with two linear patterned patches. The angle between the patches with respect to the center of the sphere is $\theta = 2\pi/5$. (i) Patchy sphere with two linear patterned patches; $\theta = 2\pi/6$. (j) Patchy sphere with patch of double rings. The rings are shifted off the equatorial plane by $\sin\varphi = \sin(\pi/6)/\sin(\pi/5)$. (k) Patchy sphere with patch of double rings at $\sin\varphi = \sin(\pi/6)/\sin(\pi/4)$. (l) Patchy sphere with patch of double rings at $\sin\varphi = \sin(\pi/6)/\sin(\pi/3)$. (m) Triangle plate with patches on the three edges. (n) Top face of patchy triangle plate with linear patterned patches. Bottom face is flipped around a vertical axis with respect to the top vertex. (o) Top face of patchy triangle plate with V-shaped patches on the two faces. (p) Bottom face of patchy particles in 1o.

both the distance between particles and relative orientations of particles. Such models are well suited to spherical particles with symmetric, regular patches, but are cumbersome for modeling nonspherical particles or irregular patches. An important advantage of our model at the expense of considering additional “atoms” is that modification of the model to arbitrary shapes requires no modification of any force fields, but simply a straightforward change in the particle geometry. The “atoms” comprising the particles may be assigned arbitrary interactions to model attractive or repulsive patches for the particular system under consideration, at any level of detail required. In this way, directional, anisotropic interactions are very simply and flexibly included.

We use Brownian dynamics, a stochastic molecular dynamics method, to simulate an isothermal system in which solvent is included implicitly through the choice of interaction potentials and drag and thermal noise terms.^{30,31} At each time step, frozen subunits move together as a rigid object using the method of quaternions.^{30,31} Each of the simulations is carried out at a fixed volume fraction $\phi = NV_0/V$ of particles in a cubic simulation box to which periodic boundaries are applied, where N is the number of particles, V_0 is the volume of a single particle, and V is the total system volume. The system sizes are small enough to achieve equilibration in a reasonable amount of time and large enough to avoid finite size effects in the local structure. Structures

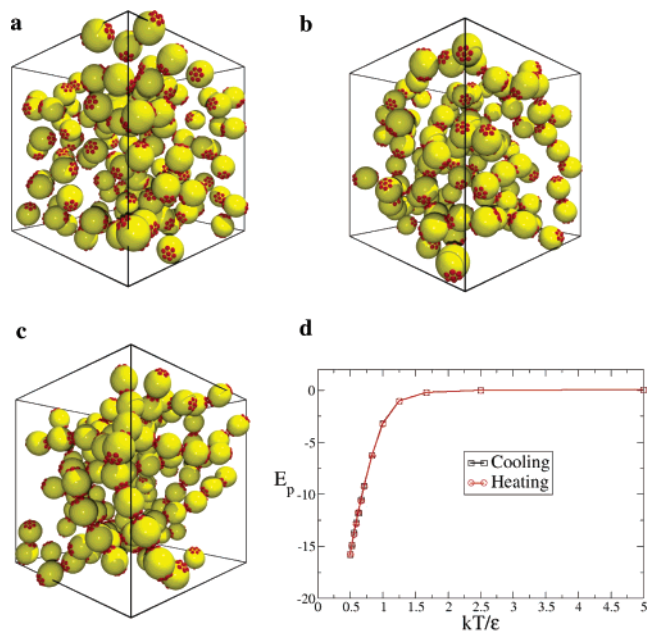


Figure 2. Equilibrium structures formed by the patchy spheres in Figure 1a. (a) Disordered state formed by 120 patchy spheres. Volume fraction of spheres $\phi = V_{\text{spheres}}/V_{\text{system}} = 0.20$. Number of beads in each sphere $N_f = 90$, diameter of spheres $D = 5\sigma$, number of beads in patches $N_{\text{pat}} = \text{number of patches} \times \text{number of beads in each patch} = 2 \times 7$, dimensionless temperature $kT/\epsilon = 2.5$. (b) Short chains formed at $kT/\epsilon = 1.0$. The other parameters are the same as in Figure 2a. (c) Long chains formed at $kT/\epsilon = 0.5$. The other parameters are the same as in Figure 2a. (d) The ensemble-averaged equilibrium potential energy per particle E_p vs kT/ϵ . The square open symbols represent equilibrium energies obtained on cooling and the square solid symbols represent those obtained on heating. The error bars indicate the ensemble standard deviation.

with one- or two-dimensional periodicity can reorient within the box so as to achieve the equilibrium spacing,^{31a} and the local arrangement of particles within “terminal” or closed structures is unaffected by the weak correlations between assembled units at the volume fractions studied. Self-assembled structures are obtained both on cooling and heating to investigate the nature of the disorder–order transition, using between four and 10 different initial disordered or ordered configurations per state point, and several different cooling and heating rates. The volume fraction and target dimensionless temperature kT/ϵ are selected to produce a specific structure based on the surface pattern of patches considered.

Figure 1 shows the patchy spherical and triangular particles studied in this work. Figure 2a–c shows the equilibrium structures formed by dilute solutions of the patchy spheres shown in Figure 1a,b at three different values of kT/ϵ . In all cases the patches are the only attractive portions of the particles. From this particular pattern of patches, we expect the particles to organize into chains in analogy with equilibrium polymerization.³² Indeed, as T decreases, we observe a continuous aggregation of particles into chains whose average size increases smoothly with decreasing T (Figure 2a–c). The equilibrium potential energy per particle E_p vs kT/ϵ calculated on cooling and heating (Figure 2d) shows

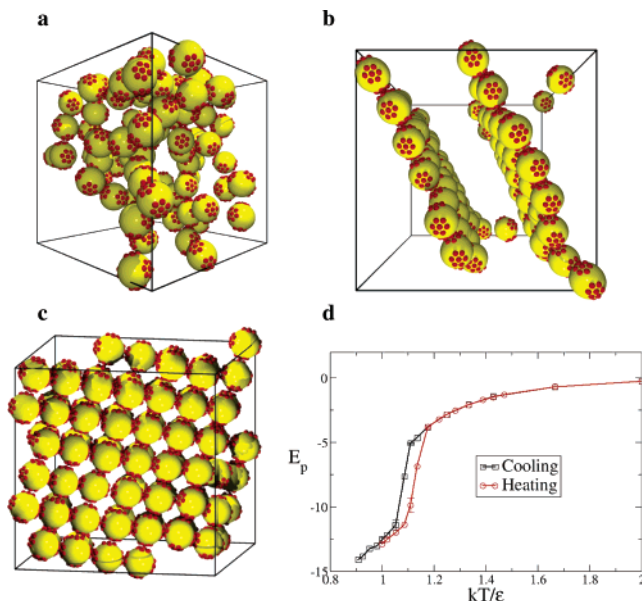


Figure 3. Assembled structures formed by patchy spheres in Figure 1c. (a) Disordered state formed by 80 patchy spheres. $\phi = 0.20$, $N_f = 90$, $D = 5\sigma$, $N_{\text{pat}} = 4 \times 7$, $kT/\epsilon = 1.67$. (b) Side view of sheets formed at $kT/\epsilon = 1.0$. The other parameters are the same as in Figure 3a. (c) Face view of sheets in Figure 3b. (d) E_p vs kT/ϵ . For the equilibrium structures, the cooling rate and starting configuration are found to be irrelevant for the final assembled structure, as expected for global, and not local, equilibrium states. The structures obtained in the transition region are metastable states.

neither hysteresis nor discontinuity, again as expected in analogy with equilibrium polymerization.

The self-assembly behavior changes when the number of patches is increased to four (Figure 3). Here, the four patches are arranged in an equatorial plane on the four vertices of a square, as in Figure 1c. Figure 3a shows the disordered, fluid phase of particles formed at $kT/\epsilon = 1.67$ and $\phi = 0.20$. When kT/ϵ decreases to 1.0, sheets form in which the particles pack in square arrays (Figure 3b–c). A plot of E_p vs kT/ϵ obtained both on cooling and heating shows an abrupt drop at $kT/\epsilon = 1.09$ (cooling) and rise at $kT/\epsilon = 1.14$ (heating), respectively, indicating a fairly sharp transition from disorder to order and vice versa. Both the sharpness of the transition and the hysteresis in the location of the transition are typical of a first-order transition.^{32a,b} This is in contrast to the continuous aggregation observed above in the formation of chains.

The above two examples considered particles with spherical, nonrecognitive patches. We next consider more complex arrangements and types of patches. Figures 4a and 4b show the assembled structures formed by spheres with attractive equatorial ring-like patches (Figure 1d,e). When $kT/\epsilon = 1.0$, the spheres form sheets as in Figure 4a,b. Instead of a square array, however, the particles pack in a hexagonal array to minimize the free energy. Figure 4c,d and 4e,f show structures again formed by spheres with equatorial ring-like patches, but where there are two types of spheres: one with a ring-like patch composed solely of molecules of type A and the other with patches composed of two kinds of molecules B and C arranged in a regular pattern (Figure 1f,g). Here, A (red) and B (green) represent complementary patches

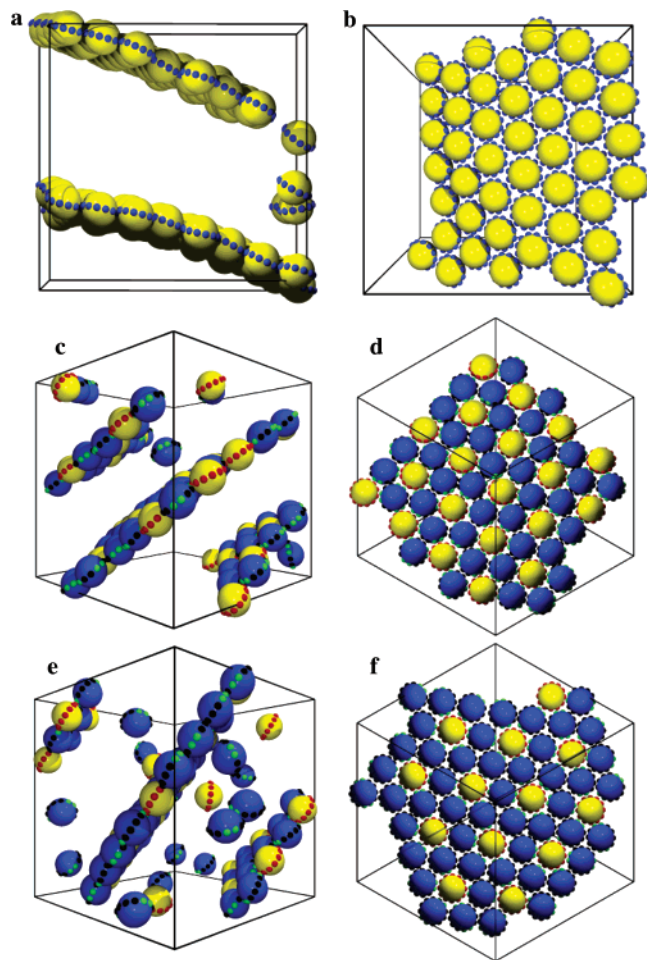


Figure 4. Equilibrium structures formed by patchy spheres with ring-like equatorial patch. (a) Side view of sheets formed by 100 patchy spheres in Figure 1d. $N_f = 58$, $D = 4\sigma$, $N_{\text{pat}} = 1 \times 12$. $\phi = 0.20$, $kT/\epsilon = 0.5$. (b) Face view of a single sheet from Figure 4a. (c) Side view of sheets formed by binary patchy spheres. The system contains 33 patchy spheres as in Figure 1d and 66 patchy spheres as in Figure 1f. The other parameters are the same as in 4a. (d) Face view of a single sheet from 4c. (e) Side view of sheets formed by binary patchy spheres. The system contains 25 patchy spheres as in Figure 1d and 75 patchy spheres as in Figure 1g. The other parameters are the same as in 4a. (f) Face view of a single sheet from 4e.

of molecules (such as complementary base pairs of DNA) and thus are attractive to each other but not to themselves. C (black) represent nonselective patches of molecules, and interact attractively only with themselves. Although both systems form hexagonally ordered sheets, the two kinds of patchy spheres (Figure 1f,g) arrange themselves on different sublattices within the sheet. We anticipate that the particular arrangement of particles within the sheet will depend on the fraction of the two particles and the relative range of interactions, as observed for a binary system of particles in an electrostatic field.^{33,34}

The above examples demonstrate the self-assembly of nonterminal 1D and 2D structures from particles with both selective and nonselective directional interactions. What is needed to self-assemble more complex structures characterized by a predetermined number of particles arranged in a precise way? For example, ring structures formed from

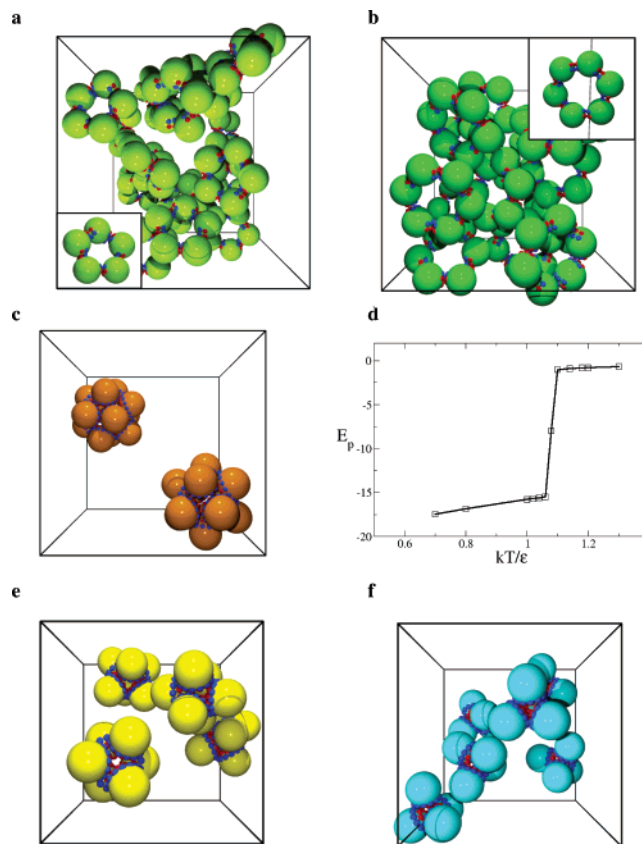


Figure 5. Equilibrium structures formed via self-assembly by patchy spheres with linear patches (Figure 1h,i) and double rings (Figure 1j,k,l). (a) Rings formed via self-assembly of patchy spheres in Figure 1h. $N_f = 90$, $D = 5\sigma$, $N_{\text{pat}} = 2 \times 6$. $\phi = 0.20$, $N_b = 90$, $kT/\epsilon = 0.33$. Each ring contains five spheres. A snapshot of a single ring is shown in the inset. (b) Rings formed via self-assembly of patchy spheres in Figure 1i. The parameters are the same as in Figure 5a. Each ring contains six spheres. A snapshot view of a single ring is shown in the inset. (c) Icosahedra formed by patchy spheres in Figure 1j. $N_f = 90$, $D = 5\sigma$, $N_{\text{pat}} = \text{number of beads in large ring} + \text{number of beads in small ring} = 15 + 12 = 27$. $\phi = 0.20$, $N_b = 24$, $kT/\epsilon = 0.88$. (d) E_p vs kT/ϵ for patchy particles in Figure 1j, which form icosahedra. The structure obtained in the transition region is likely metastable, although the structure is stable for the duration of the simulation; all other structures are independent of starting configuration and cooling rate and thus represent global equilibrium structures. (e) Square pyramids formed by patchy spheres in Figure 1k. $N_{\text{pat}} = 13 + 9 = 22$. The other parameters are the same as in Figure 5c. (f) Tetrahedra formed by patchy spheres in Figure 1l. $N_{\text{pat}} = 12 + 7 = 19$. The other parameters are the same as in Figure 5c.

nanoparticles are desirable for nanoelectronics and complex materials.³⁵ By designing two attractive patches in the equatorial plane of a spherical particle at a relative azimuthal angle $\theta < 180^\circ$, rings should be possible, but we find this to be the case only if some directionality is imparted to the patches that maintains a constant handedness in the particle arrangement. Figure 5a shows rings that self-assemble from spherical particles with two linear patches as in Figure 1h. To impart directionality, two types of molecules are included in each patch. At low T , interactions between molecules of the same type (indicated by color) are favorable and those between different molecules are unfavorable. From the position of the attractive patches in Figure 1h, we expect

that the particles will arrange into rings and each ring will contain five spheres. By changing the angle between the patches the diameter of the ring can be controlled. Figure 5b shows rings composed of six particles patterned as in Figure 1i.

By imparting directionality in the same way to ring-like patches shifted off the equatorial plane, we obtain self-assembled, complex, three-dimensional structures. Figure 5c shows icosahedra formed by spheres with a patch of double rings (Figure 1j). Although virus assembly is considerably more complicated, our results demonstrate that simple surface patterns in the interactions between particles can lead to virus-like structures.³⁶ The melting behavior shown in Figure 5d indicates the self-assembly of icosahedra occurs via a first-order transition, as found for sheets. Such transitions are also found in atomic clusters. For example, 13 argon atoms interacting via a LJ potential are known to form stable, close-packed icosahedra, and the melting behavior of these clusters shows pronounced features of a first-order transition.^{37,37a} Whereas in atomic icosahedral clusters the forces between atoms are uniform, isotropic, and spherically symmetric, the icosahedra observed here arise solely from the directionality and specificity of the forces between anisotropic patches on the surfaces of otherwise nonattractive particles. By simply altering the positions of the patches (Figure 1k,l) polyhedra such as square pyramids (Figure 5e) and tetrahedra (Figure 5f) are obtained.

Our model is easily modified to study the assembly of nonspherical particles, such as rods,^{38,39} cubes,^{40,41} and plates.^{42,43} As an example, we consider triangular plates such as those reported in ref 44. Figure 6a,b shows self-assembled structures formed from triangular plates with patches on the edges of the plates. When the three edges of the triangle are coated with patches that are attractive at low T (Figure 1m), the particles spontaneously form 2D sheets (Figure 6a) in which the particles are arranged in a triangular lattice (Figure 6b). Figure 6c,d shows structures formed from triangular plates with patches on the faces. In Figure 6c, the particles contain patches composed of two types of molecules as illustrated in Figure 1n, where same-type molecules are attractive only to each other. Again, the self-assembled structures result from the specific topology and location of the patches. By adjusting the direction and angle of the linear patches on the two particle faces, the twist direction and pitch can be controlled. Similar twisted structures have been reported in the self-assembly of millimeter scale rectangular slabs.⁴⁵ Staircase structures (Figure 6d) can be formed from triangular plates by patterning the patches as in Figure 1o,p, with two V-shaped, complementary patches on opposite faces of the plate. By tuning the distance between the two patches, the step length may be controlled.

In summary, we introduced a simple model capable of describing particles and patches of arbitrary size, shape, and material, and used molecular simulation to study their self-assembly into target structures. Our simulations predict that by coating the surfaces of particles with strongly anisotropic, highly directional, weakly interacting “patches”, complex, predictable structures such as chains (wires), sheets, rings,

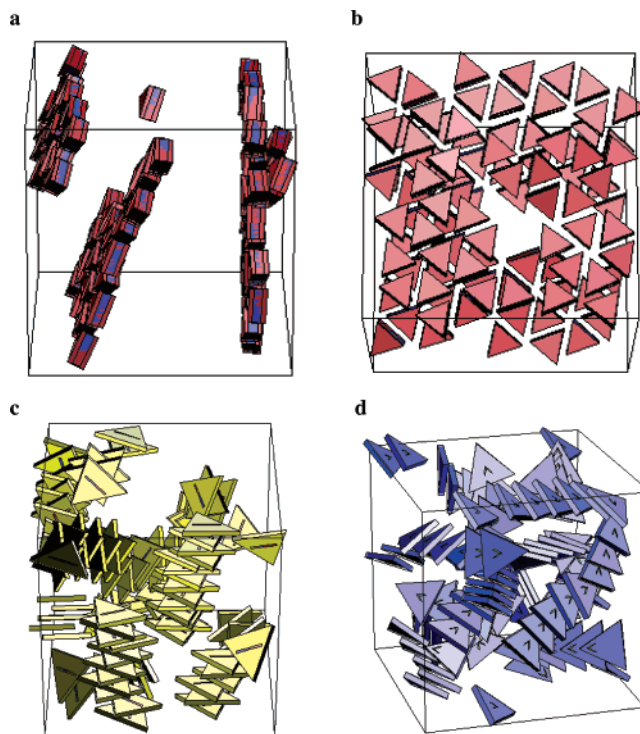


Figure 6. Equilibrium structures formed by patchy triangle plates. (a) Side view of sheets formed by patchy triangle plates in Figure 1m. $N_f = 36$, edge length of the triangle plate $L = 5\sigma$, $N_{\text{pat}} = 12$, $\phi = 0.20$, $N_b = 100$, $kT/\epsilon = 0.5$. (b) Face view of a single sheet from 6a. (c) Twisted structures formed by patchy triangle plates in Figure 1n. $N_f = 132$, $L = 13\sigma$, $N_{\text{pat}} = 2 \times 6$, $\phi = 0.20$, $N_b = 100$, $kT/\epsilon = 0.25$. (d) Staircase structures formed by patchy triangle plates in Figure 1o,p. $L = 11\sigma$, $N_{\text{pat}} = 2 \times 7$, $kT/\epsilon = 0.5$. The other parameters are the same as in Figure 6c.

icosahedra, square pyramids, tetrahedra, and twisted and staircase structures may be obtained on cooling from a disordered state. We further predict that the formation of sheets and icosahedra occurs via a first-order transition while the formation of chains is continuous and analogous to equilibrium polymerization. Many of the structures we predict here should prove useful in device fabrication. For example, the 2D arrays (sheets) of spheres with tunable lattice structures may serve as novel materials with interesting optical⁴⁶ and mechanical⁴⁷ properties. The chains, rings, and twisted and staircase assemblies may serve as basic structural units to further prepare materials with more complex structures such as tubes, helices, and 3D networks that may, in turn, serve as scaffolds or templates for assembly of electronic⁴⁸ or optical⁴⁹ components, or as channels for transport of liquids or molecules.⁵⁰ In the present study, we used relatively simple interaction potentials to describe the immiscibility between patches and particles in the interest of constructing a general, minimal model of patchy particles. Specific experimental systems may be modeled by parameterizing interactions using experimental data or, for some systems, fully atomistic simulations of one or two particles. Efforts in this direction are underway.

Acknowledgment. Financial support was provided by the Department of Energy, Grant No. DE-FG02-02ER46000. We

thank N. Kotov, R. G. Larson, M. J. Solomon, and M. A. Horsch for helpful discussions. We additionally thank C. R. Iacovella and Y. F. Shi for their help in rendering the images. We thank the University of Michigan Center for Advanced Computing for support of our computing cluster.

References

- (1) Ashoori, R. C. *Nature* **1996**, 379, 413–419.
- (2) Li, L. S.; Hu, J. T.; Yang, W. D.; Alivisatos, A. P. *Nano Lett.* **2001**, 1, 349–351.
- (3) Mihailovic, D.; Arcon, D.; Venturini, P.; Blinc, R.; Omerzu, A.; Cevc, P. *Science* **1995**, 268, 400–402.
- (4) Bowden, N. B.; Weck, M.; Choi, I. S.; Whitesides, G. M. *Acc. Chem. Res.* **2001**, 34, 231–238.
- (5) Clark, T. D.; Tien, J.; Duffy, D. C.; Paul, K. E.; Whitesides, G. M. *J. Am. Chem. Soc.* **2001**, 123, 7677–7682.
- (6) Love, J. C.; Gates, B. D.; Wolfe, D. B.; Paul, K. E.; Whitesides, G. M. *Nano Lett.* **2002**, 2, 891–894.
- (7) Paul, K. E.; Prentiss, M.; Whitesides, G. M. *Adv. Funct. Mater.* **2003**, 13, 259–263.
- (8) Jackson, A. M.; Myerson, J. W.; Stellacci, F. *Nature Mater.* **2004**, 3, 330–336.
- (9) Mirkin, C. A.; Letsinger, R. L.; Mucic, R. C.; Storhoff, J. J. *Nature* **1996**, 382, 607–609.
- (10) Parak, W. J.; Pellegrino, T.; Micheel, C. M.; Gerion, D.; Williams, S. C.; Alivisatos, A. P. *Nano Lett.* **2003**, 3, 33–36.
- (11) Banerjee, I. A.; Yu, L. T.; Matsui, H. *Nano Lett.* **2003**, 3, 283–287. [11a] Tkachenko, A. V. *Phys. Rev. Lett.* **2002**, 89, 148303–14.
- (12) Wang, Y.; Tang, T.; Liang, X.; Liz-Marzán, L. M.; Kotov, N. A. *Nano Lett.* **2004**, 4, 225–231.
- (13) Pacholski, C.; Kornowski, A.; Weller, H. *Angew. Chem., Int. Ed.* **2002**, 41, 1188–1191.
- (14) Puentes, V. F.; Krishnan, K. M.; Alivisatos, A. P. *Science* **2001**, 291, 2115–2117.
- (15) Peng, X. G.; Manna, L.; Yang, W. D.; Wickham, J.; Scher, E.; Kadavanich, A.; Alivisatos, A. P. *Nature* **2000**, 404, 59–61.
- (16) Ahmadi, T. S.; Wang, Z. L.; Green, T. C.; Henglein, A.; El Sayed, M. A. *Science* **1996**, 272, 1924–1926.
- (17) Tang, Z. Y.; Kotov, N. A.; Giersig, M. *Science* **2002**, 297, 237.
- (18) Wang, Z. L.; Harfenist, S. A.; Vezmar, I.; Whetten, R. L.; Bentley, J.; Evans, N. D.; Alexander, K. B. *Adv. Mater.* **1998**, 10, 808.
- (19) Rabani, E. *J. Chem. Phys.* **2001**, 115, 1493–1497.
- (20) Shim, M.; Guyot-Sionnest, P. *J. Chem. Phys.* **1999**, 111, 6955–6964.
- (21) Li, L. S.; Alivisatos, A. P. *Phys. Rev. Lett.* **2003**, 90, Art. No. 097402.
- (22) Kavanagh, G. M.; Clark, A. H.; Ross-Murphy, S. B. *Int. J. Biol. Macromol.* **2000**, 28, 41–50.
- (23) Laradji, M.; Toxvaerd, S.; Mouritsen, O. G. *Phys. Rev. Lett.* **1996**, 77, 2253–2256.
- (24) Bhattacharya, A.; Mahanti, S. D.; Chakrabarti, A. *Phys. Rev. Lett.* **1998**, 80, 333–336.
- (25) Grest, G. S.; Lacasse, M.-D. *J. Chem. Phys.* **1996**, 105, 10583–10594.
- (26) Kern, N.; Frenkel, D. *J. Chem. Phys.* **2003**, 118, 9882–9889.
- (27) Lomakin, A.; Asherie, N.; Benedek, G. B. *Proc. Natl. Acad. Sci. U.S.A.* **1999**, 96, 9465–9468.
- (28) Haas, C.; Drenth, J.; Wilson, W. W. *J. Phys. Chem. B* **1999**, 103, 2808–2811.
- (29) Sear, R. P. *J. Chem. Phys.* **1999**, 111, 4800–4806.
- (30) Allen, M. P.; Tildesley, D. J. *Computer Simulation of Liquids*; Clarendon: Oxford, 1987.
- (31) Zhang, Z. L.; Horsch, M. A.; Lamm, M. H.; Glotzer, S. C. *Nano Lett.* **2003**, 3, 1341–1346. [31a] Larson R. G. *J. Phys. II France* **1996** vol. 6, 1441–1463.
- (32) Dudowicz, J.; Freed, K. F.; Douglas, J. F. *J. Chem. Phys.* **2003**, 119, 12645–12666. [32a] Stanley, H. E. *Introduction to phase transitions and critical phenomena*, 1971; Oxford University Press: Oxford. [32b] Hill, T. L. *Thermodynamics of Small Systems*, 1994; Dover Publications: New York.
- (33) Kolny, J.; Kornowski, A.; Weller, H. *Nano Lett.* **2002**, 2, 361–364.
- (34) Grzybowski, B. A.; Winkleman, A.; Wiles, J. A.; Brumer, Y.; Whitesides, G. M. *Nature Mater.* **2003**, 2, 241–245.
- (35) Zhou, W. L.; He, J. B.; Fang, J. Y.; Huynh, T. A.; Kennedy, T. J.; O'Connor, C. J. *J. Appl. Phys.* **2003**, 93, 7340–7342.
- (36) Schwartz, R.; Shor, P. W.; Prevelige, P. E., Jr.; Berger, B. *Biophys. J.* **1998**, 75, 2626–2636.
- (37) Beck, T. L.; Jellinek, J.; Berry, R. S. *J. Chem. Phys.* **1987**, 87, 545–554. [37a] Frantz, D. D. *J. Chem. Phys.* **1995**, 102, 3747–3768.
- (38) Li, L. S.; Walda, J.; Manna, L.; Alivisatos, A. P. *Nano Lett.* **2002**, 2, 557–560.
- (39) Busbee, B. D.; Obare, S. O.; Murphy, C. J. *Adv. Mater.* **2003**, 15, 414–416.
- (40) Sun, Y. G.; Xia, Y. N. *Science* **2002**, 298, 2176–2179.
- (41) Vaucher, S.; Fielden, J.; Li, M.; Dujardin, E.; Mann, S. *Nano Lett.* **2002**, 2, 225–229.
- (42) Kooij, F. M. V. d.; Kassapidou, K.; Lekkerkerker, H. N. W. *Nature* **2000**, 406, 868–871.
- (43) Sun, Y. G.; Mayers, B.; Xia, Y. N. *Nano Lett.* **2003**, 3, 675–679.
- (44) Malikova, N.; Pastoriza-Santos, I.; Schierhorn, M.; Kotov, N. A.; Liz-Marzán, M. *Langmuir* **2002**, 18, 3694–3697.
- (45) Oliver, S. R. J.; Clark, T. D.; Bowden, N.; Whitesides, G. M. *J. Am. Chem. Soc.* **2001**, 123, 8119–8120.
- (46) Reese, C. E.; Baltusavich, M. E.; Keim, J. P.; Asher, S. A. *Anal. Chem.* **2001**, 73, 5038–5042.
- (47) Schope, H. J.; Decker, T.; Palberg, T. *J. Chem. Phys.* **1998**, 109, 10068–10074.
- (48) Gracias, D. H.; Boncheva, M.; Omoregie, O.; Whitesides, G. M. *Appl. Phys. Lett.* **2002**, 80, 2802–2804.
- (49) Tarhan, I. I.; Watson, G. H. *Phys. Rev. Lett.* **1996**, 76, 315–318.
- (50) Whitesides, G. M. *Sci. Am.* **1995**, 273, 146–149.

NL0493500